JCTC Journal of Chemical Theory and Computation

Article

pubs.acs.org/JCTC

Comparison of Molecular Contours for Measuring Writhe in Atomistic Supercoiled DNA

Thana Sutthibutpong, Sarah A. Harris, and Agnes Noy*

Polymer IRC, School of Physics and Astronomy, University of Leeds, Leeds West Yorkshire, Leeds LS2 9JT, U.K.

Supporting Information

ABSTRACT: DNA molecular center-lines designed from atomistic-resolution structures are compared for the evaluation of the writhe in supercoiled DNA using molecular dynamics simulations of two sets of minicircles with 260 and 336 base pairs. We present a new method called WrLINE that systematically filters out local (i.e., subhelical turn) irregularities using a sliding-window averaged over a single DNA turn and that provides a measure of DNA writhe that is suitable for comparing atomistic resolution data with those obtained from measurements of the global molecular shape. In contrast, the contour traced by the base-pair origins defined by the 3DNA program largely overestimates writhe due to the helical periodicity of DNA. Nonetheless, this local modulation of the molecular axis emerges as an internal mechanism for the DNA to confront superhelical stress, where the adjustment between low and high twist is coupled to a high and low local periodicity, respectively, mimicking the different base-stacking conformational space of A and B canonical DNA forms.

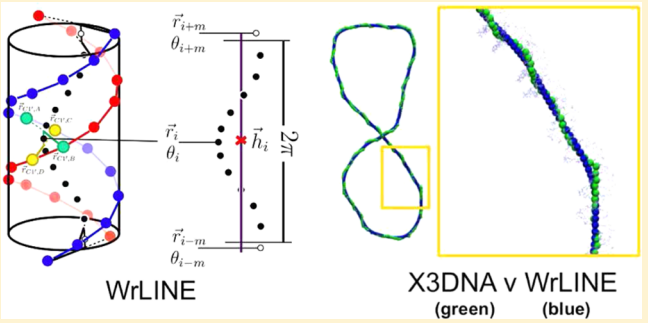

1. INTRODUCTION

DNA rarely exists in a relaxed state. Rather, it is subjected to torsional stress due to cellular processes such as transcription and replication,[1,2] and it is highly dynamic due to topoisomerase activity[3,4] and nucleosome remodelling.[5] In turn, changes in supercoiling modify the structure of DNA and can facilitate strand separation as a prerequisite for transcription initiation or replication.[6,7] Supercoiling also influences protein recognition,[8,9] the packing of the prokaryotic genome,[10] and eukaryotic chromatin structure.[11]

DNA supercoiling is quantified by the linking number (Lk), which is the number of times one strand is wrapped around the other. For a relaxed molecule with unconstrained ends, the default Lk (Lk_0) is equal to the twist (Tw), which is the number of base pairs divided by the helical repeat. However, when torsional stress is present, it can be relieved by (i) the introduction of writhe (Wr), which is the coiling of the DNA helix around itself, or (ii) by changes in the molecular helical twist (Tw): Lk = Tw + Wr. Commonly, this difference $\Delta Lk = Lk - Lk_0$ is normalized to give the superhelical density $\sigma = \Delta Lk/Lk_0$.[12]

Topoisomers (DNA molecules with the same base sequence but different Lk) of DNA circles containing a few hundred bases provide ideal systems to explore DNA topology.[13] In the laboratory, gel electrophoresis has been used to compare the degree of Wr or compaction of different minicircle topoisomers.[14−16] Atomic force microscopy and cryo-electron microscopy have both been used to visualize the global shape of these minicircles and have provided additional insight into how torsional stress is partitioned between Tw and Wr.[15−17] While there is still no experimental structure of supercoiled DNA at the atomic level due to the difficulty of crystallizing a closed DNA loop, insight into how higher order DNA structures may pack has been provided by the atomistic structure of a DNA coiled coil.[18] Fortunately, with current computational resources, atomistic simulations of circles that are sufficiently large (~300 or base pairs (bp)) that they contain more than a single persistence length of DNA are now possible. These computer models provide a fully atomistic description of supercoiled DNA structures[19] and how they are affected by environmental factors such as bound proteins or different ionic environments.[9,20,21] Therefore, there is a need for an accurate quantification of DNA supercoiling from all-atom structures that is capable of mirroring low-resolution experimental measurements, to facilitate comparisons between the two.

However, the evaluation of an appropriate helical molecular axis from an atomistic resolution structure, which is essential to quantify Wr, is nontrivial. Duplex DNA is not a simple uniform rod, but a chiral double helix, which possesses a consistent bend toward the major groove at base-pair level that imparts a periodicity in the local molecular contour.[22] Consequently, the Tw and Wr partition calculated for an atomistic structure can be sensitive to the precise center-line definition, as demonstrated by Clauvelin et. al using the GeoToC software.[23] This can give rise to artifacts, such as relaxed DNA minicircles apparently having nonzero Wr. In this article, we present a new scheme to calculate the center line of double-stranded DNA

Received: January 15, 2015
Published: May 7, 2015

DOI: 10.1021/acs.jctc.5b00035
J. Chem. Theory Comput. 2015, 11, 2768−2775

Table 1. Overview of Implicitly[a] and Explicitly[b] (in italics) Solvated DNA MD Simulations

length	Lk	R_g[c]	ΔLk	σ	Wr(WrLINE)[c]	Wr(CURVES+)[c]	Wr(3DNA)[c]
				336 bp based minicircles			
336	28	132.2 ± 11.7	−2	−0.067	−1.10 ± 0.12	−1.43 ± 0.13	+0.12 ± 0.27
336	*28*	*137.3 ± 1.6*	*−2*	*−0.067*	*−0.97 ± 0.10*	*−1.21 ± 0.11*	*+0.22 ± 0.15*
336	29	144.2 ± 12.9	−1	−0.033	−0.62 ± 0.17	−0.91 ± 0.18	+0.43 ± 0.31
340	30	153.2 ± 8.8	0	−0.012	−0.42 ± 0.21	−0.67 ± 0.22	+0.66 ± 0.38
338	30	161.0 ± 5.8	0	−0.006	−0.18 ± 0.11	−0.41 ± 0.12	+0.97 ± 0.23
336	30	170.9 ± 3.2	0	0.000	+0.05 ± 0.07	−0.20 ± 0.08	+1.05 ± 0.19
336	*30*	*169.2 ± 4.2*	*0*	*0.000*	*−0.01 ± 0.02*	*−0.20 ± 0.04*	*+0.96 ± 0.22*
334	30	165.9 ± 3.8	0	+0.006	−0.01 ± 0.07	−0.25 ± 0.09	+1.02 ± 0.20
332	30	162.3 ± 6.7	0	+0.012	+0.06 ± 0.09	−0.17 ± 0.10	+0.26 ± 0.19
336	31	157.2 ± 7.9	+1	+0.033	+0.50 ± 0.14	+0.26 ± 0.14	+1.20 ± 0.23
336	32	135.0 ± 10.0	+2	+0.067	+1.11 ± 0.12	+0.86 ± 0.12	+1.56 ± 0.21
336	*32*	*138.7 ± 1.1*	*+2*	*+0.067*	*0.96 ± 0.03*	*+0.75 ± 0.04*	*+1.37 ± 0.11*
				260 bp based minicircles			
260	22	101.1 ± 5.6	−2	−0.069	−1.08 ± 0.13	−1.36 ± 0.14	−0.43 ± 0.24
260	23	111.6 ± 6.3	−1	−0.027	−0.31 ± 0.19	−0.54 ± 0.20	+0.35 ± 0.33
266	24	131.0 ± 4.2	0	−0.007	−0.04 ± 0.11	−0.25 ± 0.11	+0.60 ± 0.18
264	24	133.5 ± 2.9	0	0.000	+0.03 ± 0.06	−0.19 ± 0.08	+0.61 ± 0.14
262	24	131.7 ± 2.5	0	+0.007	+0.11 ± 0.05	−0.11 ± 0.16	+0.62 ± 0.14
260	24	130.4 ± 3.0	0	+0.015	+0.14 ± 0.07	−0.08 ± 0.25	+0.57 ± 0.15
258	24	128.3 ± 3.1	0	+0.023	+0.16 ± 0.12	−0.02 ± 0.22	+0.57 ± 0.18
260	25	121.8 ± 7.5	+1	+0.058	+0.76 ± 0.16	0.56 ± 0.16	+1.05 ± 0.23
				20 bp linear fragments[d]			
264	24	133.5 ± 2.9	0	0.000	+0.0005 ± 0.0080	−0.0077 ± 0.0076	+0.0323 ± 0.0269
20					−0.0061 ± 0.0144	−0.0079 ± 0.0093	+0.0243 ± 0.0302
20					*−0.0024 ± 0.0091*	*−0.0062 ± 0.0050*	*+0.0189 ± 0.0203*

[a]The last 10 ns from each 20 ns trajectory were analyzed. Molecular conformations were sampled every picosecond. [b]The last 5 ns from a 6 ns trajectory for the minicircles and the last 100 ns from a 200 ns trajectory for linear fragment were considered in the analysis. Molecular configurations were sampled once every 10 ps. [c]These are averages and standard deviations. [d]Fragment extracted from the 260 bp DNA minicircle with $\sigma \approx 0$ and from linear 36mer.

that smooths local irregularities at the subturn level by systematically averaging over a full helical turn. We then evaluate how different geometry descriptions from the widely used programs 3DNA and CURVES+ affect the measurement of Wr in supercoiled DNA. While 3DNA defines a central helical contour by linking successive base pairs,[24,25] the CURVES+ software infers a curvilinear molecular contour computed by a polynomial weighting function.[26] We demonstrate using a series of minicircle topoisomers of two different sizes that our new method provides robust Wr measurements that correlate appropriately with the radius of gyration of the circles.

2. METHODS

Choice of Circle Sequences and Sizes. Five topoisomers (ΔLk = −2,−1,0,1,2) of minicircles containing 260 and 336 bp were simulated using atomistic molecular dynamics. The sequences for the 260 and 336 bp minicircles were extended from those used in the experimental work reported by Fogg et al.[16] and Zhao et. al,[27] respectively, to correct the known underestimation of relaxed DNA twist in the parmBSC0 force field[28] with parmOL3 corrections for χ dihedral[29] (33.5° compared to 34.5°).[13] To precisely quantify the DNA σ, four additional simulations were performed where the minicircle size was varied: so circles containing 258, 262, 264, and 266 bps (for the 260 Lk = 24 minicircle) and 330, 332, 334, and 338 (for the 336 Lk = 30 minicircle) were also performed. All molecular dynamics (MD) simulations are summarized in Table 1, and the exact sequences are provided in the Supporting Information.

Superhelical Density. The σ is the difference in the linking number between the torsionally stressed and the relaxed topoisomers (Lk − Lk_0), normalized by the total number of turns in the relaxed molecule (Lk_0):

$$\sigma = \frac{(\mathrm{Lk} - \mathrm{Lk}_0)}{\mathrm{Lk}_0} \tag{1}$$

However, to evaluate the σ of torsionally stressed DNA circles with an extended or reduced sequence, we need to determine the Lk_0 of a relaxed DNA molecule with the same number of bps (N) as the topoisomer under consideration ($Lk_{0,N}$). This value is obtained using the relaxed helical repeat (b_0) of the least compact topoisomer (e.g., the one with the maximum radius of gyration) containing N_0 bp and Lk_0 turns:

$$b_0 = \frac{N_0}{\mathrm{Lk}_0}, \qquad \mathrm{Lk}_{0,N} = \frac{N}{b_0}. \tag{2}$$

Then, σ for a circle close in length to the truly relaxed circle is given by

$$\sigma = \frac{(\mathrm{Lk}_N - \mathrm{Lk}_{0,N})}{\mathrm{Lk}_{0,N}} \tag{3}$$

DOI: 10.1021/acs.jctc.5b00035
J. Chem. Theory Comput. 2015, 11, 2768−2775

Simulations of Minicircles in Implicit Solvent. Linear starting structures were built using the NAB module[30] in AmberTools 1.5.[31] DNA planar circles with a specific linking number and uniform twist were then constructed using an in-house program.[20] The amber99[32,33] force field with the parmBSC0 correction for α/γ[28] and the parmOL3 correction for χ dihedrals[29] were used to describe the DNA. The generalized Born/solvent accessible area (GB/SA) implicit solvent model was used with the Hawkins, Cramer, and Truhlar pairwise generalized Born method,[34] together with the parameters recommended for DNA by Tsui and Case,[35] as previously.[20,21,36] The systems were minimized, thermalized, and equilibrated using our standard equilibration protocol.[20] The final structures were subject to 20 ns production MD simulation at constant temperature (300 K) and with a salt concentration of 0.2 M determined by the Debye−Huckel screening parameter. A cutoff of 100 Å was used for nonbonded force field terms to exceed the Debye−Huckel screening length. SHAKE[37] was used for hydrogen atoms in conjunction with an integration time step of 2 fs. Additionally, we impose restraints for the Watson−Crick canonical H-bonds in the production runs. MD simulations were performed using the Sander module of AMBER11.[31] Configurations were sampled every 1 ps. Only the last 10 ns of the simulations were analyzed; this was performed using the PTRAJ module in the AmberTools 1.5 package.

Simulations of Minicircles in Explicit Solvent. Three topoisomers from the 336-based minicircles (Lk = 28, 30, and 32) were chosen for explicit solvent simulations. To select the starting structure, we performed clustering analysis using the average linkage algorithm within PTRAJ for the implicitly solvated DNA trajectories. Representative structures of the most populated clusters then were solvated in rectangular boxes containing ∼700 000 water molecules; 672 Na^+ counterions were added to neutralize the DNA charges along with excess salt (1250 Na^+/Cl^- ion pairs) to make these calculations compatible with the 0.2 M salt concentration in the implicit solvent. TIP3P[38] water molecules together with Smith and Dang ions model[39] were used to represent solvent molecular interactions. Systems were energy-minimized, thermalized (T = 300 K), and equilibrated using a standard protocol,[19,40]followed by a final re-equilibration of 1 ns. The final structures were subject to 5 ns of MD simulation at constant temperature (300 K) and pressure (1 atm) using periodic boundary conditions and particle mesh Ewald.[41] The Settle algorithm[42] was used to constrain bond lengths and angles of water molecules, and P-LINCS[43] was used for all other bond lengths in conjunction with an integration time step of 2 fs. These simulations were performed using the Gromacs-4 computer program,[44] and the final structures were carefully visualized to ensure that rotation of the solute was not significant compared to the size of the simulation box over the time scale of the MD.

Simulations of Unconstrained Linear Fragment. A 36mer fragment was selected from the 260 bp minicircle to compare Wr between the constrained and unconstrained DNA. A fragment length of 20 bp, which is ∼1.5−2 DNA turns after removing ends effects, allows us to explore the effect that the local DNA periodicity has on the Wr measure. To avoid the bending present at the apexes of the plectoneme, the fragment was chosen to be close to the crossing point of the minicircle (see Figure 1). The linear starting structure was solvated implicitly and explicitly for running MD simulations of an unconstrained linear piece of DNA. Both systems were set up, minimized, and equilibrated following the protocols described in previous sections.

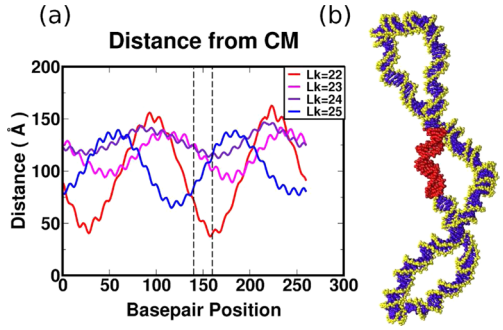

Figure 1. (a) Distances between centers of mass (CM) for every residue and the CM of the whole 260 bp minicircle. Values reported here are averages over last 10 ns of the corresponding MD simulations. Dashed lines indicate the residues spanning the linear 20 bp fragment. (b) Snapshot of a negatively supercoiled topoisomer with the chosen linear 20 bp fragment highlighted. Small distances in (a) indicate locations near the crossing point, while large distances indicate locations in the apexes. .

WrLINE Model for DNA Molecular Contour. A diagrammatic representation of the WrLINE molecular contour is provided in Figure 2. Our definition of this DNA molecular contour is built from a set of reference points $\vec{h}_i$, each associated with a dinucleotide step. The definition of each $\vec{h}_i$ is an average over the helical turn surrounding the corresponding bp step to smooth local molecular irregularities.

Initially, for every dinucleotide step, we extract the midpoint $\vec{r}_i$ by averaging the C1′ atoms ($\vec{r}_{C1'}$) of the four bases (A, B, C, and D) forming that bp step (see Figure 2b):

$$\vec{r}_i = \frac{\vec{r}_{C1',A} + \vec{r}_{C1',B} + \vec{r}_{C1',C} + \vec{r}_{C1',D}}{4} \tag{4}$$

The bp step twist θ_i is calculated by using the midpoint between two base-pair C1′ atoms $\vec{r}_{A,B}$ and $\vec{r}_{C,D}$ that define the local helical axis $\vec{z}_i$ and its perpendicular plane Z (see Figure 2a,b):

$$\vec{z}_i = \vec{r}_{A,B} - \vec{r}_{C,D} \tag{5}$$

The vectors $\vec{y}_{A,B}$ and $\vec{y}_{C,D}$ pointing to C1′ atoms are then projected to the plane Z ($\vec{y}_{A,B;Z}$ and $\vec{y}_{C,D;Z}$), and the bp twist θ_i is defined by the angle between them (see Figure 2b):

$$\theta_i = \cos^{-1}(\vec{y}_{A,B;Z} \cdot \vec{y}_{C,D;Z}) \tag{6}$$

Then, the number of bps ($2m$) necessary to construct the helical turn around the bp step i is obtained through the Θ_m parameter, which is the summation of the associated bp step twists (θ):

$$\Theta_m = \theta_i + \sum_{k=1}^{m} (\theta_{i+k} + \theta_{i-k}) \tag{7}$$

with the condition that

$$\Theta_m > 2\pi > \Theta_{m-1} \tag{8}$$

being:

$$\Theta_{m-1} = \theta_i + \sum_{k=1}^{m-1} (\theta_{i+k} + \theta_{i-k}) \tag{9}$$

which can be rearranged to give

DOI: 10.1021/acs.jctc.5b00035
J. Chem. Theory Comput. 2015, 11, 2768−2775

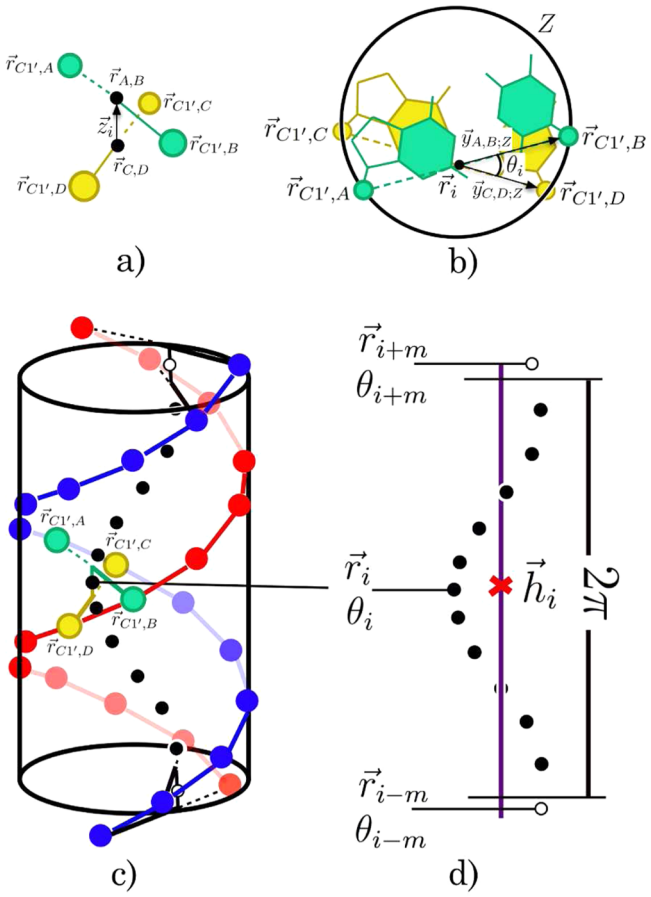

Figure 2. Schematic diagram for the WrLINE molecular contour. (a, b) A bp step with its corresponding midpoint $\vec{r}_i$ and twist θ_i. The first one is specified by the four C1′ atoms coordinates $\vec{r}_{C1'}$. The latter one is defined through the bases midpoints $\vec{r}_{A,B}$ and $\vec{r}_{C,D}$, the local helical axis $\vec{z}_i$ and its perpendicular plane Z, and the $\vec{y}_{A,B;Z}$ and $\vec{y}_{C,D;Z}$, which point to C1′ atoms on plane Z. (c, d) Side views of a helical turn denoted by a cylinder, with all internal midpoints $\vec{r}_i$ (black dots) and flanking $\vec{r}_{i+m}$ and $\vec{r}_{i-m}$ (white dots), which are weighted to correct for the excess twist (θ_{i+m}, θ_{i-m}). These sets of points are averaged for the evaluation of a reference point $\vec{h}_i$ (red cross) for the molecular contour.

$$\Theta_m = \Theta_{m-1} + (\theta_{i+m} + \theta_{i-m}) \tag{10}$$

Afterward, a weighting factor w is evaluated to scale down the relative importance of the two base-pair steps ($i + m$ and $i - m$) at the outside boundary (see Figure 2c,d) by

$$2\pi = \Theta_{m-1} + w(\theta_{i+m} + \theta_{i-m}) \tag{11}$$

where w can be written as

$$w = \frac{2\pi - \Theta_{m-1}}{\theta_{i+m} - \theta_{i-m}} = \frac{2\pi - \Theta_{m-1}}{\Theta_m - \Theta_{m-1}} \tag{12}$$

Finally, all the midpoints within the helical turn (r_i, black dots in Figure 2) together with the two weighted flanking midpoints ($\vec{r}_{i+m}$ and $\vec{r}_{i-m}$, white dots in Figure 2) are averaged to produce the reference point $\vec{h}_i$ (red cross in Figure 2c) associated with the dinucleotide step i

$$\vec{h}_i = \frac{1}{2(m + w) - 1}(\vec{r}_i + w(\vec{r}_{i+m} + \vec{r}_{i-m}) + \sum_{k=1}^{m-1} (\vec{r}_{i+k} + \vec{r}_{i-k})) \tag{13}$$

the whole set of which represents the DNA molecular contour. Additional information is available in the Supporting Information.

Writhe Calculations. The pathway of the DNA molecular center line was obtained by (i) the origin of the coordinate frame assigned locally to every bp by 3DNA,[24,25] (ii) the curvilinear molecular contour obtained by CURVES+,[26] and (iii) the set of reference points ($\vec{h}$) that define our smooth model in WrLINE (see above). Then, Wr was calculated by the summation of the Gauss integral[20] (which gives equivalent results to GeoToc[23] (see Figure S1 in the Supporting Information) but can be used on a linear helical fragment). For the 36mer linear fragments, the central 32 bp were used to extract the global CURVES+ and WrLINE molecular contours, respectively. End effects were eliminated by subsequently considering only the central 20 bp. For 3DNA (which is not influenced by the global environment), reference frames were evaluated directly for the central 20 bp.

3. RESULTS AND DISCUSSION

Global Minicircle Structures. We performed a series of implicit solvent simulations for a 260- and 336-based DNA minicircles (see Table 1). Since these circles contain approximately two persistence lengths of DNA, they were sufficiently long to allow plectonemes to form in response to supercoiling, in spite of the high levels of bending required to form the apexes. The use of the GB/SA implicit solvent model allowed a satisfactory exploration of conformational space[35] due to the enhanced sampling that can be achieved when solvent friction is neglected. Although more approximate, implicit solvent models have been shown to provide a comparable description of supercoiled DNA to explicitly solvated calculations in monovalent salt, so long as the DNA does not contain defects in the double helix.[36] For this reason, restraints were imposed on the canonical H-bonds in our simulations. Moreover, we considered only relatively low levels of superhelical stress (ΔLk $\pm$ 2, which lies inside the range of $\pm$0.07 found in DNA isolated from *E. coli* cells[45]) in which melting is only expected to occur at special sequence motifs.[6] Within the first 5 ns of implicitly solvated MD, the trajectories show a rapid transition of the initially planar circle into a writhed conformation with helical parameters and dihedral angles within the range expected for a B-type structure (see Figure 3 and Supporting Information, Figure S2). No kinking or other forms of disruptions were detected in the base stacking interactions in any of the trajectories. Finally, to demonstrate that the results are independent of our choice of solvent model, we performed short (5 ns) simulations in explicit solvent for representative structures sampled from the 336 bp ΔLk = −2,0, +2 by clustering (see Methods Section), and no significant alterations were observed (see Table 1).

Identification of the $\sigma \approx 0$ Minicircle. The radius of gyration (R_g) was used as a criterion to determine the most-relaxed supercoiled topoisomer with $\sigma \approx 0$. Although the correlation between the R_g and Wr is not univocal (see Figure 3c), R_g represents the degree of writhing in simulated DNA circles with an overall correlation coefficient of 0.72 for

DOI: 10.1021/acs.jctc.5b00035
J. Chem. Theory Comput. 2015, 11, 2768−2775

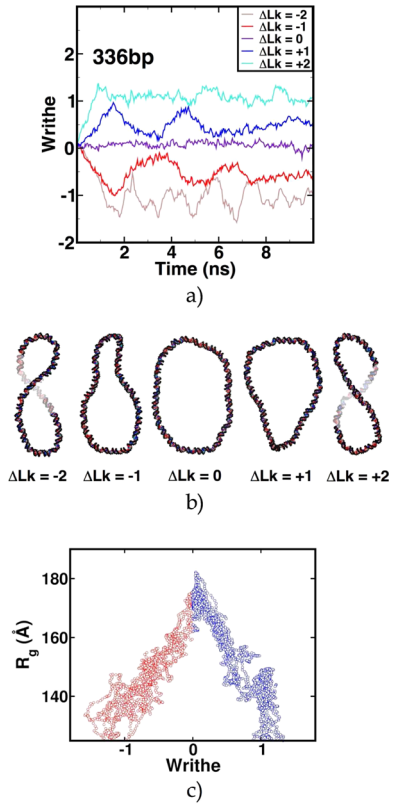

Figure 3. (a) Variation of Wr along the first 5 ns using the WrLINE molecular contour, (b) snapshots sampled from the MD trajectories showing the global shape, and (c) scatter plots showing the correlation between R_g and Wr obtained by WrLINE for the different 336 bp minicircle topoisomers.

negatively supercoiled DNA and 0.85 for positively supercoiled DNA. Moreover, because R_g is an indicator of global compactness, it reflects the experimental Wr estimates inferred by different gel electrophoretic mobilities[14,46] or by the general shapes observed by Cryo-EM.[15−17] Additionally, the design of minicircles with a specific Lk number is extremely difficult due to the inherent complexity of extracting the exact value of the local twist for the individual DNA base steps. As pointed out by Olson and co-workers, subtle differences in the definition of the DNA molecular axis can give rise to alterations in the apparent twist.[23] Moreover, two contrasting geometric approximations are possible; the first calculates the so-called supercoiled twist, which mimics the helical periodicity inferred from DNA cyclization experiments. The second is based on the local "bp twist" traditionally extracted from X-ray or NMR structures and atomistic simulations.[47] Furthermore, a detailed analysis of high-resolution experimental structures has shown that the local twist is also highly sequence-dependent. Average local twist values as low as 29.7° · bp^{-1} have been reported for AG steps, but twists as high as 41.8° · bp^{-1} have been seen in TA and CA steps.[48] The potential for twist variability is further enhanced by the influence of the nearest neighbor sequences surrounding a given dinucleotide step[49] and also by the presence of sequence motifs such as A-tracts,[50] which have special mechanical properties that are emergent over longer stretches of DNA.

As is shown in Table 1, we found that topoisomers Lk = 24 and Lk = 30 for 260 and 336 minicircles, respectively, presented the biggest R_g, allowing us to establish that these are the most relaxed topoisomers (ΔLk = 0). To obtain a value for the σ as close to zero as possible, four additional simulations of minicircles constructed by altering the number of bp within the most relaxed topoisomer were performed (see Table 1 and the Supporting Information). The minicircle with the largest R_g was assigned as the one with $\sigma \approx 0$ and used as a reference to determine the σ of the rest of the DNA loops (see Methods Section and Table 1).

Evaluation of the Writhe. Figure 4 compares the Wr calculated as a function of the σ from DNA molecular contours

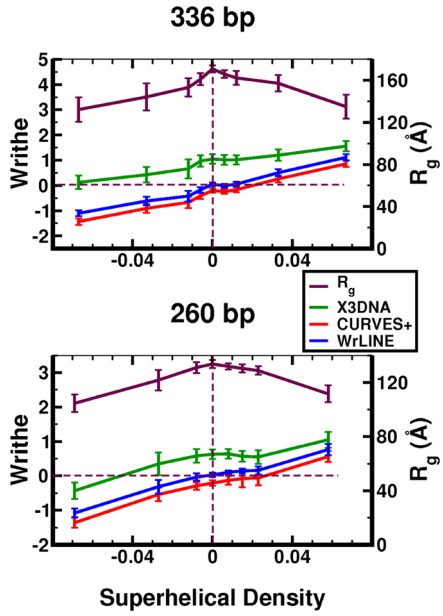

Figure 4. Radius of gyration and writhe (in DNA turns) measurements for the 260 and 336 bp implicitly solvated minicircles as a function of the superhelical density (see Table 1). Values reported here are averages over last 10 ns of the corresponding MD simulations, and the associated standard deviations are given as error bars.

as defined by X3DNA (in green) CURVES+ (red) and WrLINE (blue). While CURVES and WrLINE both predict Wr ≈ 0 close to the designated ΔLk = 0 topoisomer, the estimation of Wr = 0 from X3DNA is displaced toward more compact, negatively supercoiled topoisomers, and lies somewhere in between the ΔLk = −1 and −2 topoisomers for both DNA minicircle systems. Additional simulations exploring $\sigma \approx 0$ allowed us to discriminate between the behavior of CURVES+ and WrLINE in the design of the circle contour. At the maximum R_g, the Wr calculated from CURVES+ is slightly underestimated (by −0.19 ± 0.08 and −0.20 ± 0.08 for the 260 and 336 bp minicircles, respectively), while our new molecular contour description provided values very close to zero (+0.03 ± 0.06 and +0.05 ± 0.07 for the 260 and 336 bp minicircles, respectively; see Table 1 and Figure 4). Although the underestimation of the Wr calculated from the CURVES+ molecular contours is small, it is critical to an accurate assignment of the σ, and therefore our understanding of the Tw/Wr balance. As an illustration, Figure 4 shows that with the CURVES+ definition of the DNA molecular contour, the Wr calculated for the ΔLk = 0 and ΔLk = +1 336 bp (σ = +0.033) are very similar, whereas R_g for ΔLk = 0 of this circle is detectably larger than for the overtwisted loop.

CURVES+ and 3DNA Molecular Contours Exhibit Local Periodicity. A visualization of the molecular axes obtained by the three schemes provides insight into the

DOI: 10.1021/acs.jctc.5b00035
J. Chem. Theory Comput. 2015, 11, 2768−2775

geometric reasons for the different measurements obtained for Wr (see Figure 5). The 3DNA molecular contour executes a

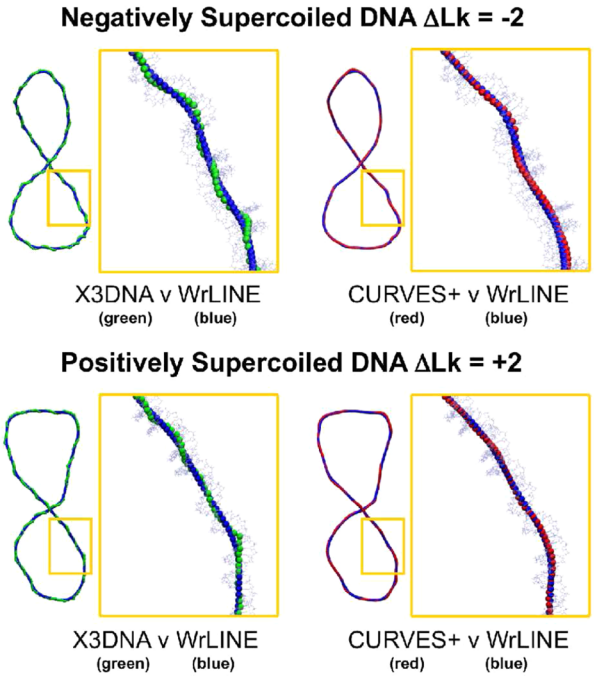

Figure 5. Molecular conformations sampled from the implicitly solvated 336 bp Lk = −2,+2 trajectories where WrLINE and CURVES +/3DNA geometrical descriptions for helical axis are compared.

local right-handed toroidal path in phase with the DNA helix for both positively and negatively supercoiled minicircles that produces a systematic overestimate of the Wr, whereas the axis defined by CURVES+ has a subtle left-handed toroidal shape, which produces a slight underestimation of the Wr. Thus, for each toroidal turn, a small amount of positive Wr (3DNA) or negative Wr (CURVES+) is introduced and accumulates. To confirm this finding, we analyzed implicitly and explicitly solvated simulations (see Table 1 and Figure 6) of a 20mer linear fragment extracted from the minicircle crossing points (to avoid any chiral bend associated with the plectonemic apexes), and obtained results consistent with our analysis of the implicitly solvated minicircle DNA, confirming that the calculated Wr was independent of the solvation model or the bending stress in small loops.

In 3DNA, the reference frames for each base pair are defined solely by their individual positions. Consequently, they capture the local periodicity of DNA, which originates from the basal curvature toward the major groove at the dinucleotide level.[22,51] Similarly, the oscillations present in the graphs shown in Figure 1a indicate that this intrinsic modulation of the bp arrangements are reflected in the distances measured between the centers-of-mass of individual base pairs and that of the whole DNA molecule. While the single bp reference frames and the curvilinear molecular contours defined by 3DNA and CURVES +, respectively, are entirely appropriate for calculations of most DNA bp properties, including the analysis of ion distributions[52] or protein-directed DNA bends,[53] WrLINE is more appropriate for the calculation of Wr, which is a global property of the whole DNA loop.

New Insights from 3DNA Molecular Contours. Figure 4 reveals that while the Wr discrepancy between the CURVES+

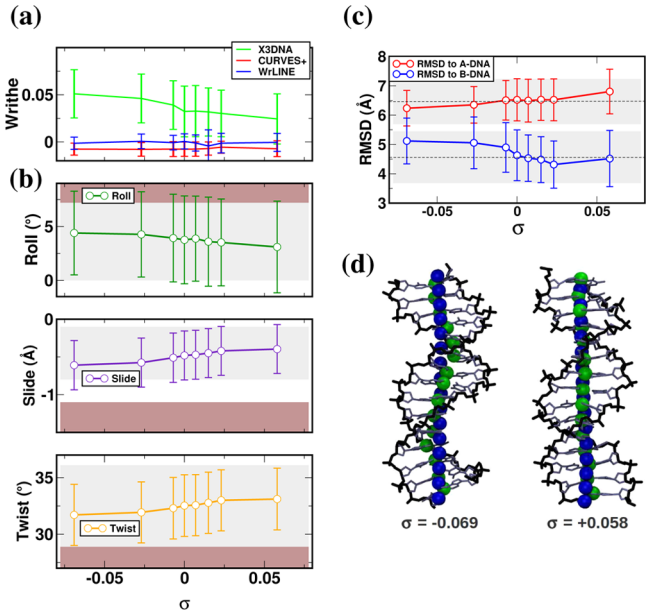

Figure 6. Wr (a), representative helical parameters (roll, twist, and slide) (b), and RMSD with respect to canonical A and B DNA forms (c) of the 20 bp DNA fragment extracted from the 260 bp minicircles constrained at different superhelical densities. In (b), values are compared with RNA (brown shading) and DNA (gray shading) simulations databases,[55,56] showing only half standard deviation for purposes of clarity. In (c), the RMSD for the unconstrained 20 bp fragment trajectory in implicit solvent was added as a frame of reference (gray shaded area). (d) Molecular structures indicating the WrLINE (in blue) and X3DNA (in green) molecular contours of the 20 bp DNA fragment constrained at different superhelical densities. Values reported here are averages over last 10 ns, and the associated standard deviations are given as error bars.

and WrLINE models has a similar magnitude throughout the range of σ investigated, the difference in the Wr calculated using 3DNA and WrLINE decreases with increasing σ. A careful visual comparison of the molecular contours calculated with 3DNA and WrLINE (see Figure 6) shows that the local periodicity captured by 3DNA is reinforced in negatively supercoiled relative to positively supercoiled DNA. This accounts for the counterintuitive result obtained with 3DNA (shown in Figure 6a) that shows that for a small linear (20mer) fragment the Wr decreases with increasing σ. Moreover, Figure 6b suggests that this "local Wr" identified by 3DNA provides an intrinsic molecular mechanism to absorb part of the torsional stress, in which twist reduction is coupled to a major-groove bend (or roll increment) in negatively supercoiled DNA, and in which high twist is coupled to a decrease in the major-groove bend in positively supercoiled DNA. These adjustments of the base-stacking in response to the superhelical stress mimic those associated with the B-to-A transition (although the structural parameters remain within the regime expected for B-DNA; see Figure 6), as also described by Randall et al.[54] So although the 3DNA molecular contour is not appropriate for calculations of global DNA Wr, it does provide useful quantification of the local toroidal Wr, which could be revealed as a novel mechanical mechanism used by duplex DNA to adjust to an imposed superhelical stress.

DOI: 10.1021/acs.jctc.5b00035
J. Chem. Theory Comput. 2015, 11, 2768−2775

4. CONCLUDING REMARKS

A series of implicitly solvated MD simulations of 260 and 336 bp minicircles has been used as test systems for quantifying the global shape of supercoiled DNA using different DNA center lines. The most-relaxed supercoiled topoisomer with $\sigma \approx 0$ was determined using the global compactness as an independent criterion. We have developed and tested a new algorithm called WrLINE that uses a sliding window averaged over a single DNA turn to smooth local irregularities inherent in the helical DNA duplex structure. WrLINE thereby provides a Wr value of zero for $\sigma = 0$ minicircle, whereas previous calculation methods do not. Thus, WrLINE is able to use atomistic-resolution structures to provide Wr values appropriate for comparison with any available experimental measurement of the global shape of DNA topoisomers. The 3DNA reference framework, which is defined solely by individual bp position, offers a quantification of the local periodicity and reveals that local writhe can provide a mechanism to absorb part of the torsional stress for negatively supercoiled DNA. Our analysis reveals that negatively supercoiled DNA presents a stronger local periodicity than positively supercoiled DNA, which is reminiscent of the different toroidal twist present in A and B canonical forms, respectively.

■ ASSOCIATED CONTENT

Ⓢ Supporting Information

The exact sequences of all DNA circles, comparison of writhe measurements using GeoToC or the summation approximation of the Gauss Integral Method, and structural information on sampled DNA. The Supporting Information is available free of charge on the ACS Publications website at DOI: 10.1021/acs.jctc.5b00035. For calculations, the code is available at http://ccpforge.cse.rl.ac.uk/gf/project/wrline.

■ AUTHOR INFORMATION

Corresponding Author

*E-mail: a.noy@leeds.ac.uk.

Notes

The authors declare no competing financial interest.

■ ACKNOWLEDGMENTS

This work was supported by the Biotechnology and Biological Sciences Research Council [Grant No. BB/I019294/1]. T.S. was funded by the Thai Ministry of Science and Technology. We acknowledge C. Laughton for providing the code to circularize the DNA, and T. Maxwell and A. Bates for their helpful comments on the manuscript. We thank the HECBiosim and ARC Leeds for computational resources.

■ REFERENCES

(1) Wang, J. C.; Lynch, A. S. *Curr. Opin. Gen. Dev.* **1993**, *3*, 764−768.
(2) Kouzine, F.; Gupta, A.; Baranello, L.; Wojtowicz, D.; Ben-Aissa, K.; Liu, J.; Przytycka, T. M.; Levens, D. *Nat. Struct. Mol. Biol.* **2013**, *20*, 396−403.
(3) Chen, S. H.; Chan, N.-L.; Hsieh, T.-s. *Annu. Rev. Biochem.* **2013**, *82*, 139−170.
(4) Baranello, L.; Kouzine, F.; Levens, D. *Transcription* **2013**, *4*, 232−237.
(5) Zivanovic, Y.; Goulet, I.; Revet, B.; Bret, M. L.; Prunell, A. *J. Mol. Biol.* **1988**, *200*, 267−285.
(6) Levens, D.; Benham, C. J. *Phys. Biol.* **2011**, *8*, 035011.
(7) Naughton, C.; Corless, S.; Gilbert, N. *Transcription* **2013**, *4*, 162−166.
(8) Fogg, J. M.; Randall, G. L.; Pettitt, B. M.; Sumners, D. W. L.; Harris, S. A.; Zechiedrich, L. *Q. Rev. Biophys.* **2012**, *45*, 257−299.
(9) D'Annessa, I.; Coletta, A.; Sutthibutpong, T.; Mitchell, J.; Chillemi, G.; Harris, S.; Desideri, A. *Nucleic Acids Res.* **2014**, *42*, 9304−9312.
(10) Postow, L.; Hardy, C. D.; Arsuaga, J.; Cozzarelli, N. R. *Genes Dev.* **2004**, *18*, 1766−1779.
(11) Naughton, C.; Avlonitis, N.; Corless, S.; Prendergast, J. G.; Mati, I. K.; Eijk, P. P.; Cockroft, S. L.; Bradley, M.; Ylstra, B.; Gilbert, N. *Nat. Struct. Mol. Biol.* **2013**, *20*, 387−397.
(12) Bates, A. D.; Maxwell, A. *DNA Topology;* Oxford University Press: Oxford, U.K., 2005.
(13) Bates, A. D.; Noy, A.; Piperakis, M. M.; Harris, S. A.; Maxwell, A. *Biochem. Soc. Trans.* **2013**, *41*, 565−570.
(14) Zivanovic, Y.; Goulet, I.; Prunell, A. *J. Mol. Biol.* **1986**, *192*, 645−660.
(15) Bednar, J.; Furrer, P.; Stasiak, A.; Dubochet, J.; Egelman, E. H.; Bates, A. D. *J. Mol. Biol.* **1994**, *235*, 825−847.
(16) Fogg, J. M.; Kolmakova, N.; Rees, I.; Magonov, S.; Hansma, H.; Perona, J. J.; Zechiedrich, E. L. *J. Phys.: Condens. Matter* **2006**, *18*, S145−S159.
(17) Amzallag, A.; Vaillant, C.; Jacob, M.; Unser, M.; Bednar, J.; Kahn, J. D.; Dubochet, J.; Stasiak, A.; Maddocks, J. H. *Nucleic Acids Res.* **2006**, *34*, e125.
(18) Campos, J. L.; Urpí, L.; Sanmartín, T.; Gouyette, C.; Subirana, J. A. *Proc. Natl. Acad. Sci. U.S.A.* **2005**, *102*, 3663−3666.
(19) Mitchell, J. S.; Laughton, C. A.; Harris, S. A. *Nucleic Acids Res.* **2011**, *39*, 3928−3938.
(20) Harris, S. A.; Laughton, C. A.; Liverpool, T. B. *Nucleic Acids Res.* **2008**, *36*, 21−29.
(21) Mitchell, J. S.; Harris, S. A. *Phys. Rev. Lett.* **2013**, *110*, 148105.
(22) Noy, A.; Golestanian, R. *Phys. Rev. Lett.* **2012**, *109*, 228101.
(23) Clauvelin, N.; Olson, W. K.; Tobias, I. *J. Chem. Theory Comput.* **2012**, *8*, 1092−1107.
(24) Lu, X.-J.; Olson, W. *Nucleic Acids Res.* **2003**, *31*, 5108−5121.
(25) Lu, X.-J.; Hassan, M. A. E.; Hunter, C. A. *J. Mol. Biol.* **1997**, *273*, 668−680.
(26) Lavery, R.; Moakher, M.; Maddocks, J. H.; Petkeviciute, D.; Zakrzewska, K. *Nucleic Acids Res.* **2009**, *17*, 5917−5929.
(27) Zhao, N.; Fogg, J. M.; Zechiedrich, L.; Zu, Y. *Gene Ther.* **2011**, *18*, 220−224.
(28) Pérez, A.; Marchán, I.; Svozil, D.; Cheatham, T. E.; Laughton, C. A.; Orozco, M. *Biophys. J.* **2007**, *92*, 3817−3829.
(29) Krepl, M.; Zgarbová, M.; Stadlbauer, P.; Otyepka, M.; Banás, P.; Koca, J.; Cheatham, T. E.; Jurecka, P.; Sponer, J. *J. Chem. Theory Comput.* **2012**, *8*, 2506−2520.
(30) Macke, T.; Case, D. *In Molecular Modeling of Nucleic Acids;* Leontes, N., SantaLucia, J., Eds.; American Chemical Society: Washington, DC, 1998.
(31) Case, D.; Darden, T.; Cheatham, T.; Simmerling, C.; Wang, J.; Duke, R.; Luo, R.; Walker, R.; Zhang, W.; Merz, K.; Roberts, B.; Wang, B.; Hayik, S.; Roitberg, A.; Seabra, G.; Kolossváry, I.; Wong, K.; Paesani, F.; Vanicek, J.; Liu, J.; Wu, X.; Brozell, S.; Steinbrecher, T.; Gohlke, H.; Cai, Q.; Ye, X.; Wang, J.; Hsieh, M.-J.; Cui, G.; Roe, D.; Mathews, D.; Seetin, M.; Sagui, C.; Babin, V.; Luchko, T.; Gusarov, S.; Kovalenko, A.; Kollman, P. *AMBER11;* University of California: San Francisco, CA, 2010.
(32) Cornell, W. D.; Cieplak, P.; Bayly, C. I.; Gould, I. R.; Kenneth, M.; Merz, J.; Ferguson, D. M.; Spellmeyer, D. C.; Fox, T.; Caldwell, J. W.; Kollman, P. A. *J. Am. Chem. Soc.* **1995**, *17*, 5179−5197.
(33) Cheatham, T. E.; Cieplak, P.; Kollman, P. A. *J. Biomol. Struct. Dyn.* **1999**, *16*, 845−862.
(34) Hawkins, G. D.; Cramer, C. J.; Truhlar, D. G. *J. Phys. Chem.* **1996**, *100*, 19824−19839.
(35) Tsui, V.; Case, D. A. *Biopolymers* **2000**, *56*, 275−291.
(36) Mitchell, J.; Harris, S. *Prog. Theor. Phys. Supplement* **2011**, *191*, 96−108.
(37) Ryckaert, J.-P.; Ciccotti, G.; Berendsen, H. J. C. *J. Comput. Phys.* **1977**, *23*, 327−341.

DOI: 10.1021/acs.jctc.5b00035
J. Chem. Theory Comput. 2015, 11, 2768−2775

(38) Jorgensen, W. L.; Chandrasekhar, J.; Madura, J. D.; Impey, R. W.; Klein, M. L. *J. Chem. Phys.* **1983**, *79*, 926−935.
(39) Smith, D. E.; Dang, L. X. *J. Chem. Phys.* **1994**, *100*, 3757−3766.
(40) Noy, A.; Golestanian, R. *J. Phys. Chem. B* **2010**, *114*, 8022−8031.
(41) Darden, T.; York, D.; Pedersen, L. *J. Chem. Phys.* **1993**, *98*, 10089−10092.
(42) Miyamoto, S.; Kollman, P. *J. Comput. Chem.* **1992**, *13*, 952−962.
(43) Hess, B. *J. Chem. Theory Comput.* **2008**, *4*, 116−122.
(44) Hess, B.; Kutzner, C.; van der Spoel, D.; Lindahl, E. *J. Chem. Theory Comput.* **2008**, *4*, 435−447.
(45) Zechiedrich, E. L.; Khodursky, A. B.; Bachellier, S.; Schneider, R.; Chen, D.; Lilley, D. M. J.; Cozzarelli, N. R. *J. Biol. Chem.* **2000**, *275*, 8103−8113.
(46) Vetcher, A. A.; McEwen, A. E.; Abujarour, R.; Hanke, A.; Levene, S. D. *Biophys. Chem.* **2010**, *148*, 104−111.
(47) Britton, L. A.; Olson, W. K.; Tobias, I. *J. Chem. Phys.* **2009**, *131*, 245101.
(48) Dans, P. D.; Pérez, A.; Faustino, I.; Lavery, R.; Orozco, M. *Nucleic Acids Res.* **2012**, *40*, 10668−10678.
(49) Lavery, R.; Zakrzewska, K.; Beveridge, D. L.; Bishop, T. C.; Case, D. A.; Cheatham, T. E.; Dixit, S. B.; Jayaram, B.; Lankas, F.; Laughton, C.; Maddocks, J. H.; Michon, A.; Osman, R.; Orozco, M.; Pérez, A.; Singh, T.; Spackova, N.; Sponer, J. *Nucleic Acids Res.* **2010**, *38*, 299−313.
(50) Drsata, T.; Spacková, N.; Jurecka, P.; Zgarbová, M.; Sponer, J.; Lankas, F. *Nucleic Acids Res.* **2014**, *42*, 7383−7394.
(51) Goodsell, D. S.; Dickerson, R. E. *Nucleic Acids Res.* **1994**, *22*, 5497−5503.
(52) Lavery, R.; Maddocks, J. H.; Pasi, M.; Zakrzewska, K. *Nucleic Acids Res.* **2014**, *42*, 8138−8149.
(53) Blanchet, C.; Pasi, M.; Zakrzewska, K.; Lavery, R. *Nucleic Acids Res.* **2011**, *39*, W68−W73.
(54) Randall, G. L.; Zechiedrich, L.; Pettitt, B. M. *Nucleic Acids Res.* **2009**, *37*, 5568−5577.
(55) Noy, A.; Luque, F. J.; Orozco, M. *J. Am. Chem. Soc.* **2008**, *130*, 3486−3496.
(56) Pasi, M.; et al. *Nucleic Acids Res.* **2014**, *42*, 12272−12283.

DOI: 10.1021/acs.jctc.5b00035
J. Chem. Theory Comput. 2015, 11, 2768−2775